[redacted]

Copy
RM L53J01a

NACA

RESEARCH MEMORANDUM

WIND-TUNNEL INVESTIGATION OF THE EFFECTS OF STEADY ROLLING ON THE AERODYNAMIC LOADING CHARACTERISTICS OF A 45° SWEPTBACK WING AT HIGH SUBSONIC SPEEDS

By James W. Wiggins and Richard E. Kuhn

Langley Aeronautical Laboratory
Langley Field, Va.

[redacted]

NATIONAL ADVISORY COMMITTEE
FOR AERONAUTICS

WASHINGTON
November 6, 1953

[redacted]

[redacted]

NATIONAL ADVISORY COMMITTEE FOR AERONAUTICS

RESEARCH MEMORANDUM

WIND-TUNNEL INVESTIGATION OF THE EFFECTS OF STEADY ROLLING ON THE AERODYNAMIC LOADING CHARACTERISTICS OF A 45° SWEPTBACK WING AT HIGH SUBSONIC SPEEDS

By James W. Wiggins and Richard E. Kuhn

SUMMARY

An investigation has been conducted in the Langley high-speed 7- by 10-foot tunnel to determine the effect of steady rolling on the aerodynamic loading characteristics of a 45° sweptback wing of aspect ratio 4 in combination with a fuselage. The investigation covered Mach numbers of 0.70, 0.85, and 0.91 at angles of attack up to 13°.

The results indicate that the loss in damping in roll previously noted for this wing is due to stalling of the tip sections. The effects of rolling velocity on the span load distribution can be satisfactorily estimated if measured pressure-distribution data in pitch are available.

INTRODUCTION

An investigation of the damping-in-roll characteristics of a number of swept wings (ref. 1) indicated a serious loss of damping at high subsonic speeds in the moderate angle of attack range (8° to 13°). Accordingly, an investigation of the distribution of pressure on one of the wings (45° sweep, aspect ratio 4) while rolling was undertaken in order to obtain a better understanding of the factors contributing to the loss of damping.

This paper presents only the load distributions in steady roll at Mach numbers of 0.70, 0.85, and 0.91. The effects of a fence on the loading characteristics at a Mach number of 0.85 are also included. The pressure-distribution characteristics in pitch for this wing are presented in reference 2.

In order to expedite the publication of these results, they are presented here without detailed analysis or discussion.

[redacted]

COEFFICIENTS AND SYMBOLS

The coefficients and symbols used in the present paper are defined as follows:

M	Mach number
R	Reynolds number
c	local wing chord, ft
c_{av}	average wing chord, S/b, ft
M.A.C.	mean aerodynamic chord, $\frac{2}{S}\int_0^{b/2} c^2 dy$, ft
b	wing span, ft
S	wing area, sq ft
α	angle of attack, deg
p	rolling velocity measured about an axis parallel with the relative wind, radians/sec
$\frac{pb}{2V}$	wing-tip helix angle, radians
V	free-stream velocity
c_n	section normal-force coefficient
$\Delta\left(\frac{c_n c}{c_{av}}\right)$	increment of spanwise loading coefficient due to rolling
$C_{l_p} = \frac{\partial C_l}{\partial \frac{pb}{2V}}$	per radian (force data presented about an axis parallel to the relative wind; pressure data presented about the body axis)
$\frac{Y}{b/2}$	spanwise station

[redacted]

MODEL AND APPARATUS

A drawing of the wing-fuselage configuration tested in shown in figure 1 and a tabulation of the fuselage ordinates is presented in reference 3. The wings were of composite construction consisting of a steel core and a bismuth-tin covering to give the desired contour. One hundred and fifteen static-pressure orificies were located in the upper and lower surfaces of the wing, distributed along five spanwise stations parallel to the plane of symmetry (20, 60, and 95 percent semispan on the right wing and 40 and 80 percent semispan on the left wing). The wing was mounted to the fuselage in a midwing position with zero dihedral and zero incidence. The brass fences (fig. 1) were disposed symmetrically on the wing and mounted so that the mounting clips did not protrude above the wing surface.

The model was tested on the forced roll support system (ref. 4) as shown in figures 2 and 3. The model was rotated about an axis parallel to the relative wind and the angle of attack was changed by the use of offset sting adapters as shown in figure 3.

A pressure-switch assembly (fig. 4) with eight NACA miniature electrical pressure gages (ref. 5) was installed in the fuselage to transmit the pressure-distribution data from the rolling wing. The eletrical signals from the pressure gages were taken through the slip rings and brushes of the forced-roll apparatus. Because of the limited number of slip rings, it was necessary to use a gang of special pressure switches geared together to connect the pressure orifices in the wing to the electrical gages in successive groups. The pressure data were recorded on a multiple-channel recording galvanometer.

TESTS AND CORRECTIONS

The tests were conducted in the Langley high-speed 7- by 10-foot tunnel at Mach numbers of 0.70, 0.85, and 0.91. The blocking corrections which were applied to the Mach number were determined by the method of reference 6. The Reynolds number (based on the mean aerodynamic chord of the wing) increased from 2.7×10^6 to 3×10^6 for Mach numbers from 0.70 to 0.91, respectively.

The angle of attack has been corrected for the deflection of the support system under load. The aeroelastic deflection characteristics of this wing (as determined from static loadings are presented in references 3 and 4. Corrections for aeroelastic distortion have not been applied to these data.

[redacted]

PRESENTATION OF RESULTS

The results of the investigation are presented in the following figures:

As indicated previously, the equipment for measuring the pressures while rolling is very complex and numberous possibilities for errors of leakage exist. The work involved in obtaining the data presented here proved to be very tedious and time consuming.

The span stations of 40 and 80 percent semispan were on the left wing of the model; however, for convenience, the data for these stations have been presented with the sign of $pb/2V$ reversed so that figure 5 presents data assuming all stations on the right wing. The span load distributions of figure 6 were constructed from the faired curves of figure 5.

The data of reference 1 indicated a serious loss of damping in roll for this wing at the higher angles of attack and higher Mach numbers (fig. 9 of this paper). This decrease in damping is due to a loss in the increment of section loading coefficient due to rolling at the wing tips (fig. 7 $\alpha = 8.8^\circ$) and occurs at angles of attack at which the data of reference 2 indicate these sections of the wing to be stalled. Note also that at the highest angle of attack investigated ($\alpha = 13^\circ$) the mid-span stations of the wing have lost effectiveness and the tips have regained some. For this wing, this results in a slight improvement in the damping at this angle of attack.

The fence successfully maintained the lift effectiveness of the tip sections and therefore the damping-in-roll effectiveness up to an angle of attack of about 13° ($M = 0.85$) (figs. 6 and 7). Similar gains would not be expected at higher Mach numbers however, because the effectiveness of a fence in maintaining the damping in roll and supressing the stall is known to decrease appreciably at the higher Mach numbers (refs. 1 and 2).

The procedure of reference 1, which used measured pressure-distribution-in-pitch data (ref. 2), has been used to estimate the increment of load distribution due to roll through the angle of attack range (fig. 8). Considering the difficulties experienced in obtaining the experimental pressure

distributions in roll, agreement between the distribution calculated by this procedure and the measured increments is very good, and, as indicated in reference 1, it appears that this estimating procedure may be the more practical approach in most instances. The good agreement between the method of reference 1 and the theory of reference 7 at zero angle of attack should also be noted (fig. 8).

CONCLUDING REMARKS

An investigation of the aerodynamic loading characteristics on a 45° sweptback wing of aspect ratio 4 during steady roll indicates that the loss of damping in roll previously noted for this wing is due to stalling of the tip section of the wing. Also, the effect of rolling velocity on the span load distribution can be satisfactorily estimated if measured pressure-distribution data in pitch are available.

Langley Aeronautical Laboratory,
National Advisory Committee for Aeronautics,
Langley Field, Va., September 15, 1953.

[redacted]

REFERENCES

1. Kuhn, Richard E.: Notes on Damping in Roll and Load Distributions in Roll at High Angles of Attack and High Subsonic Speeds. NACA RM L53G13a, 1953.

2. Kuhn, Richard E., Wiggins, James W., and Byrnes, Andrew L., Jr.: Wind-Tunnel Investigation of the Effects of a Fence and a Leading-Edge Notch on the Aerodynamic Loading Characteristics in Pitch of a 45° Sweptback Wing at High Subsonic Speeds. NACA RM L53H24, 1953.

3. Kuhn, Richard E., and Wiggins, James W.: Wind-Tunnel Investigation of the Aerodynamic Characteristics in Pitch of Wing-Fuselage Combinations at High Subsonic Speeds. Aspect-Ratio Series. NACA RM L52A29, 1952.

4. Kuhn, Richard E., and Wiggins, James W.: Wind-Tunnel Investigation To Determine the Aerodynamic Characteristics in Steady Roll of a Model at High Subsonic Speeds. NACA RM L52K24, 1952.

5. Patterson, John L.: A Miniature Electrical Pressure Gage Utilizing a Stretched Flat Diaphragm. NACA TN 2659, 1952.

6. Hensel, Rudolph, W.: Rectangular-Wind-Tunnel Blocking Corrections Using the Velocity-Ratio Method. NACA TN 2372, 1951.

7. Bird, John D.: Some Theoretical Low-Speed Span Loading Characteristics of Swept Wings in Roll and Sideslip. NACA Rep. 969, 1950. (Supersedes NACA TN 1839.)

8. Goodman, Alex, and Adair, Glen H.: Estimation of the Damping in Roll of Wings Through the Normal Flight Range of Lift Coefficient. NACA TN 1924, 1949.

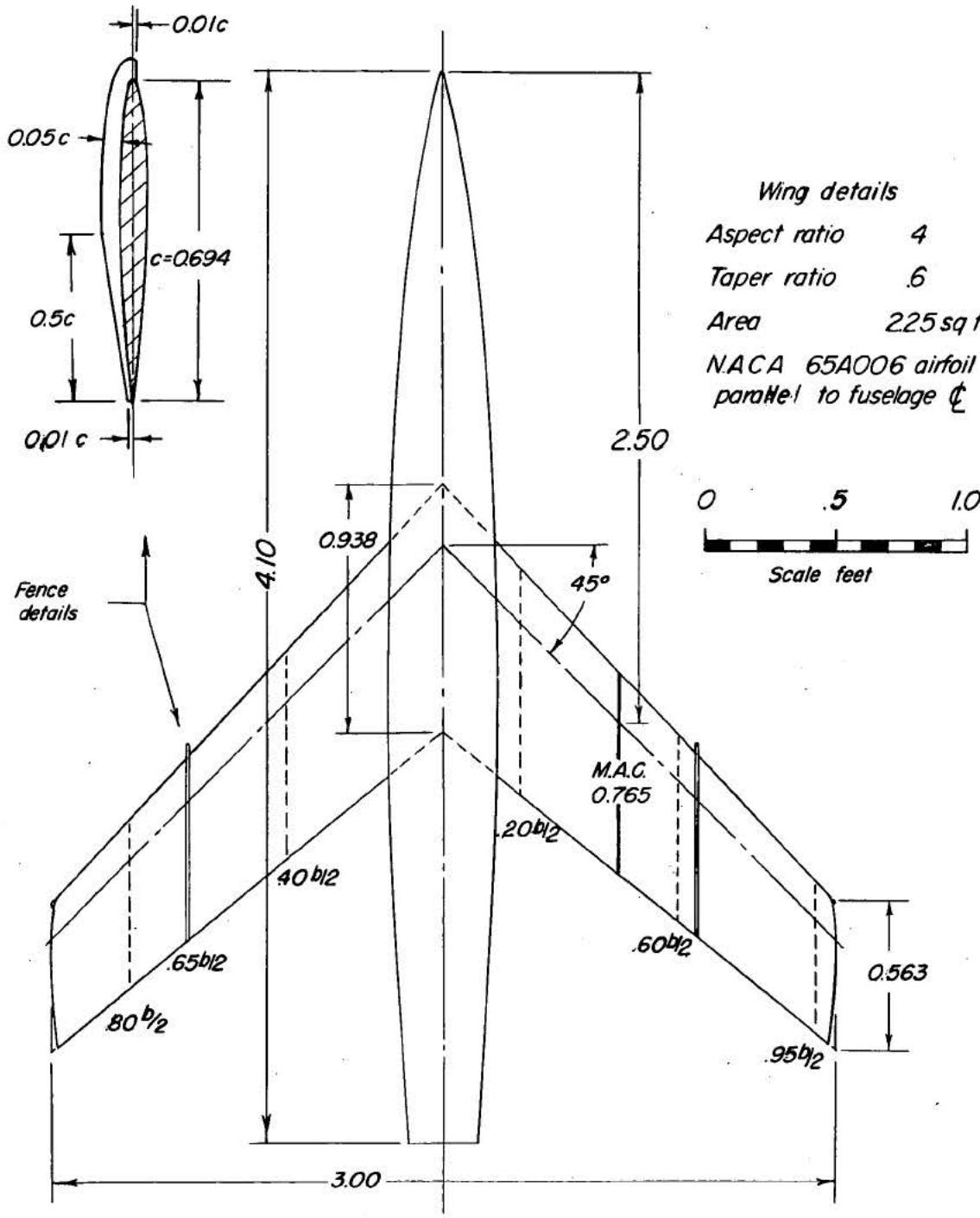

Figure 1.- Drawing of the model.

[redacted]

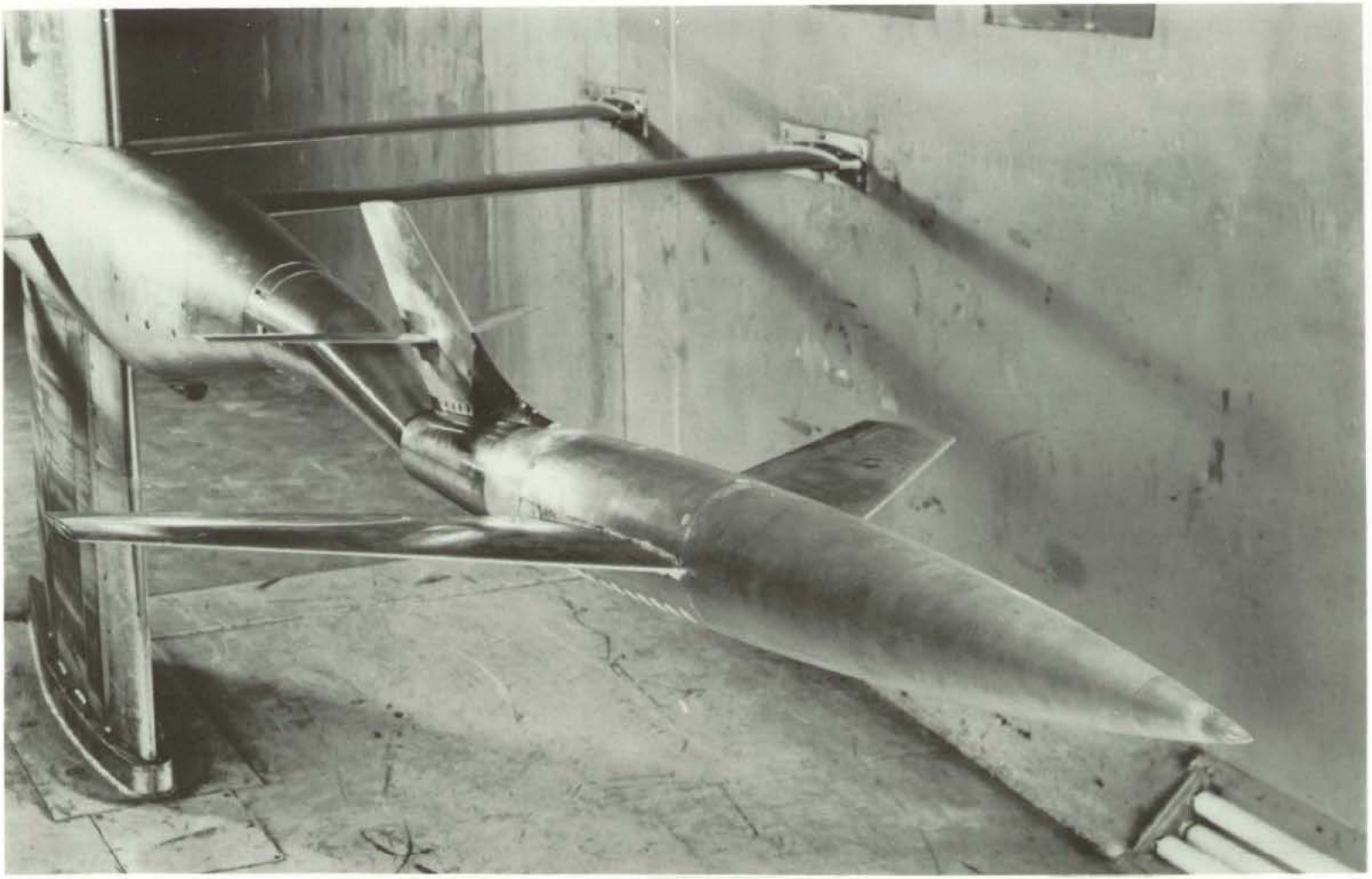

L-70081

Figure 2.- Photograph of a model installed on the forced-roll support system at an angle of attack.

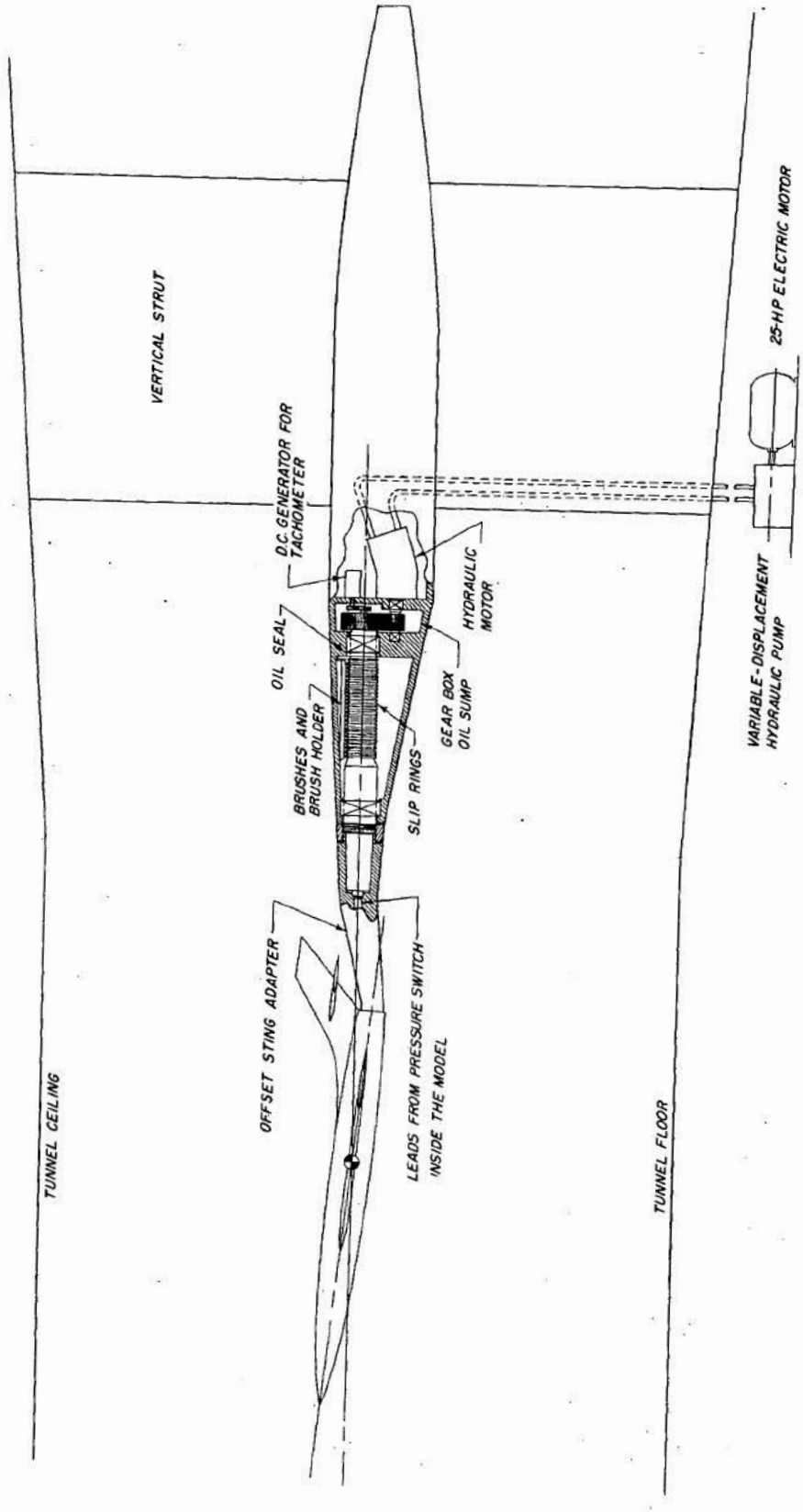

Figure 3.- General arrangement of forced-roll support system.

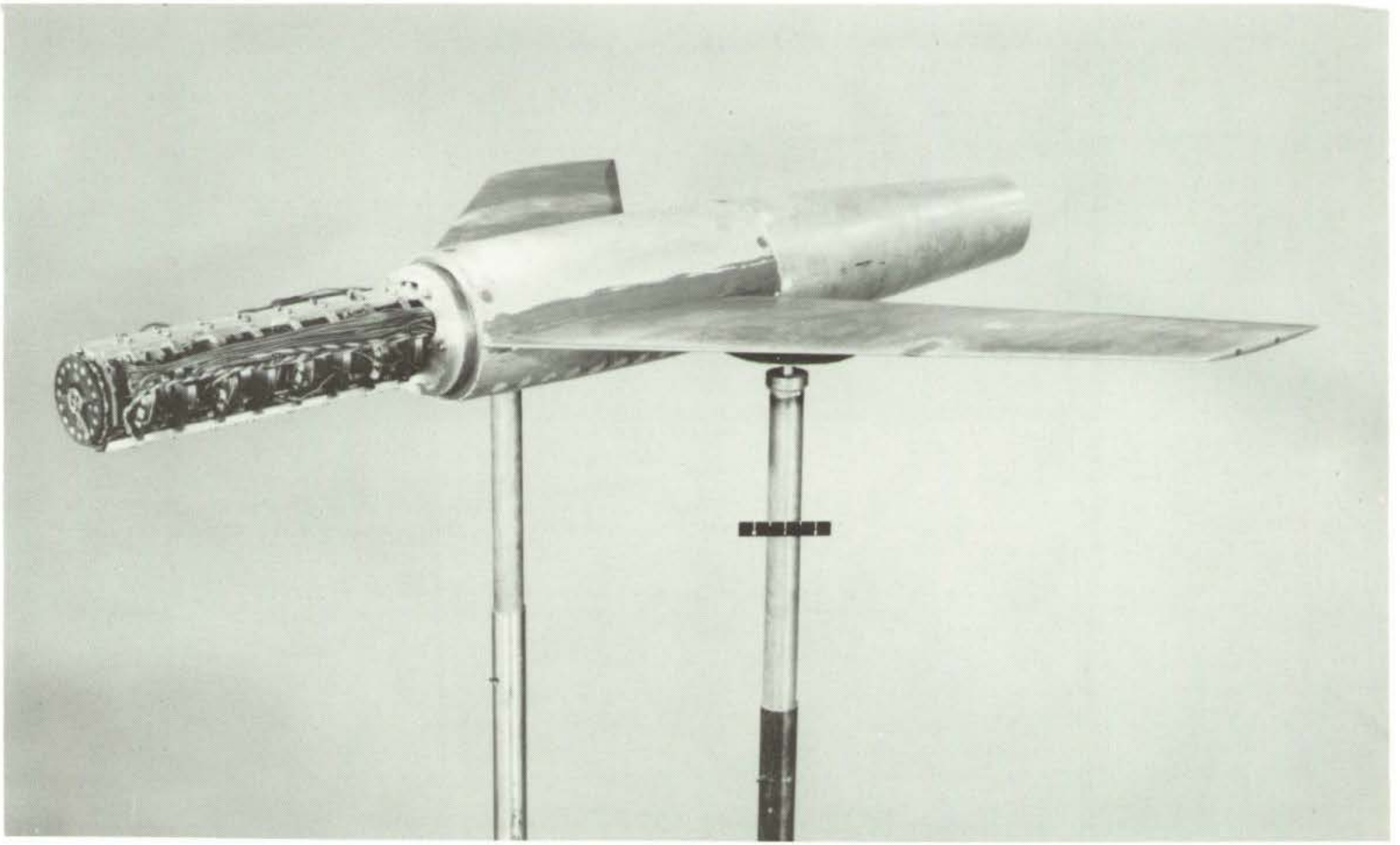

L-79572

(a) Installation in model.

Figure 4.- Photographs of pressure-switch assembly.

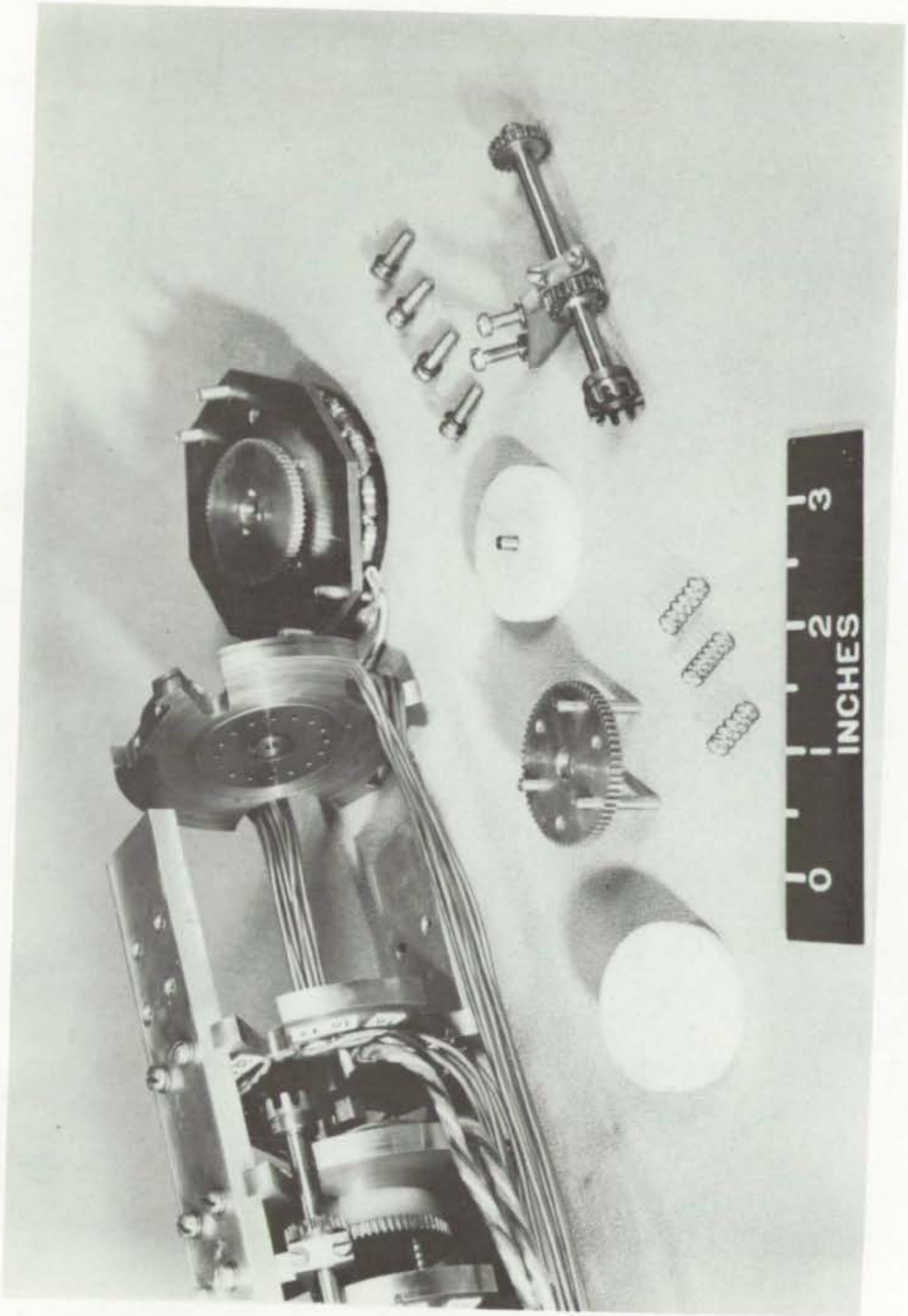

L-62793

(b) Closeup showing details of construction.

Figure 4.- Continued.

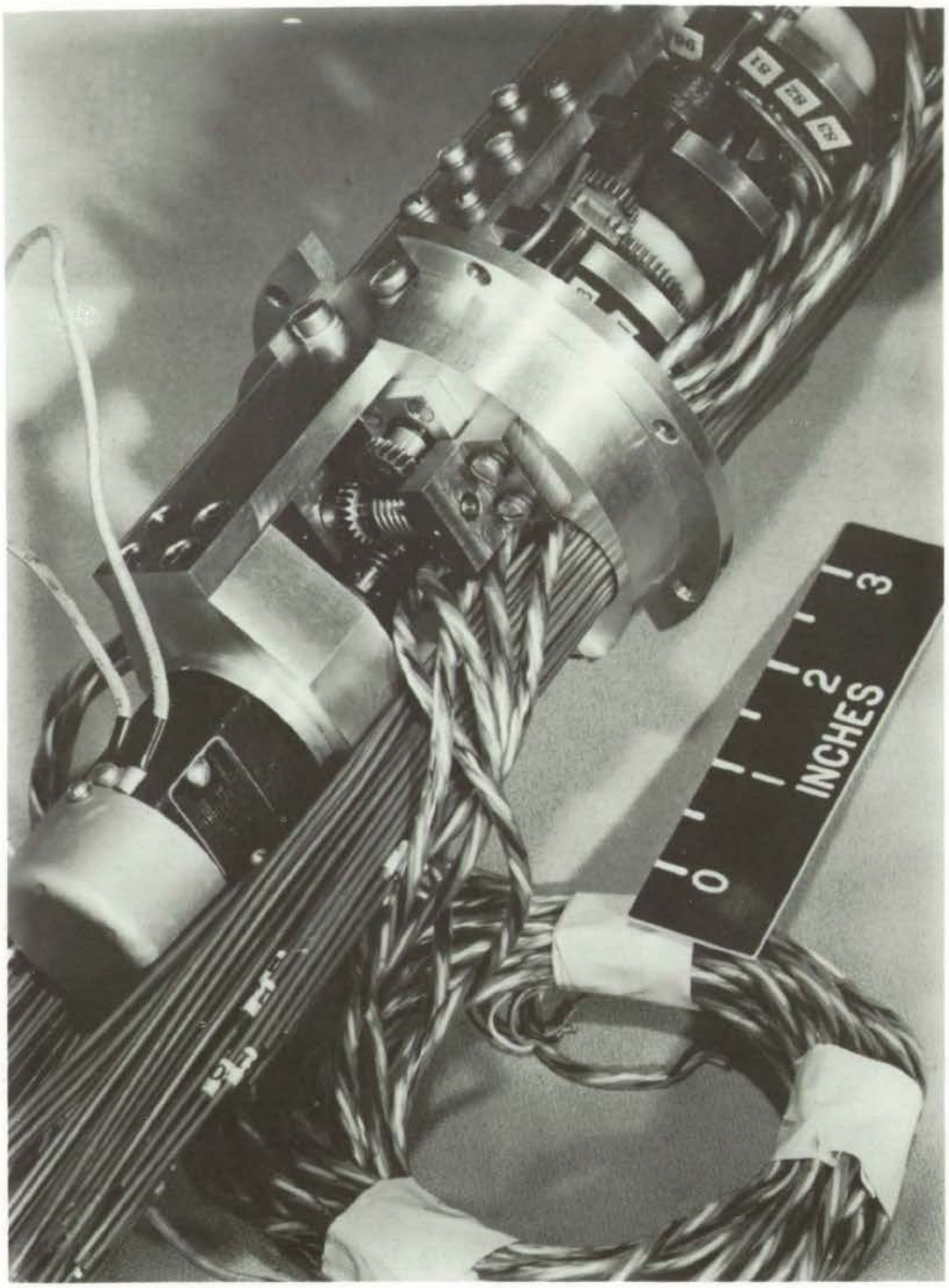

L-62790

(c) Closeup showing drive motor and reduction gearing.

Figure 4.- Concluded.

[redacted]

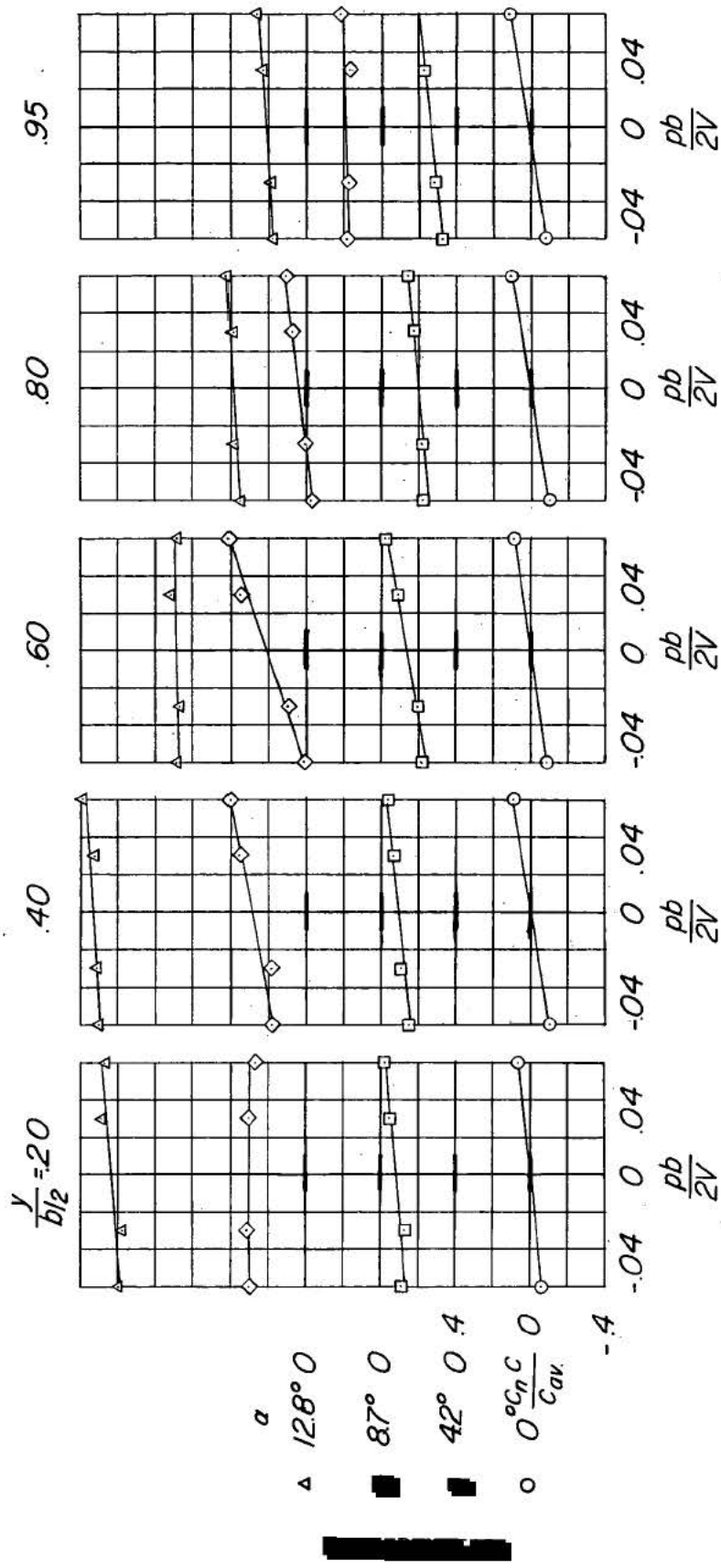

(a) M = 0.7; clean wing.

Figure 5.- Variation of span loading coefficient with rate of roll.

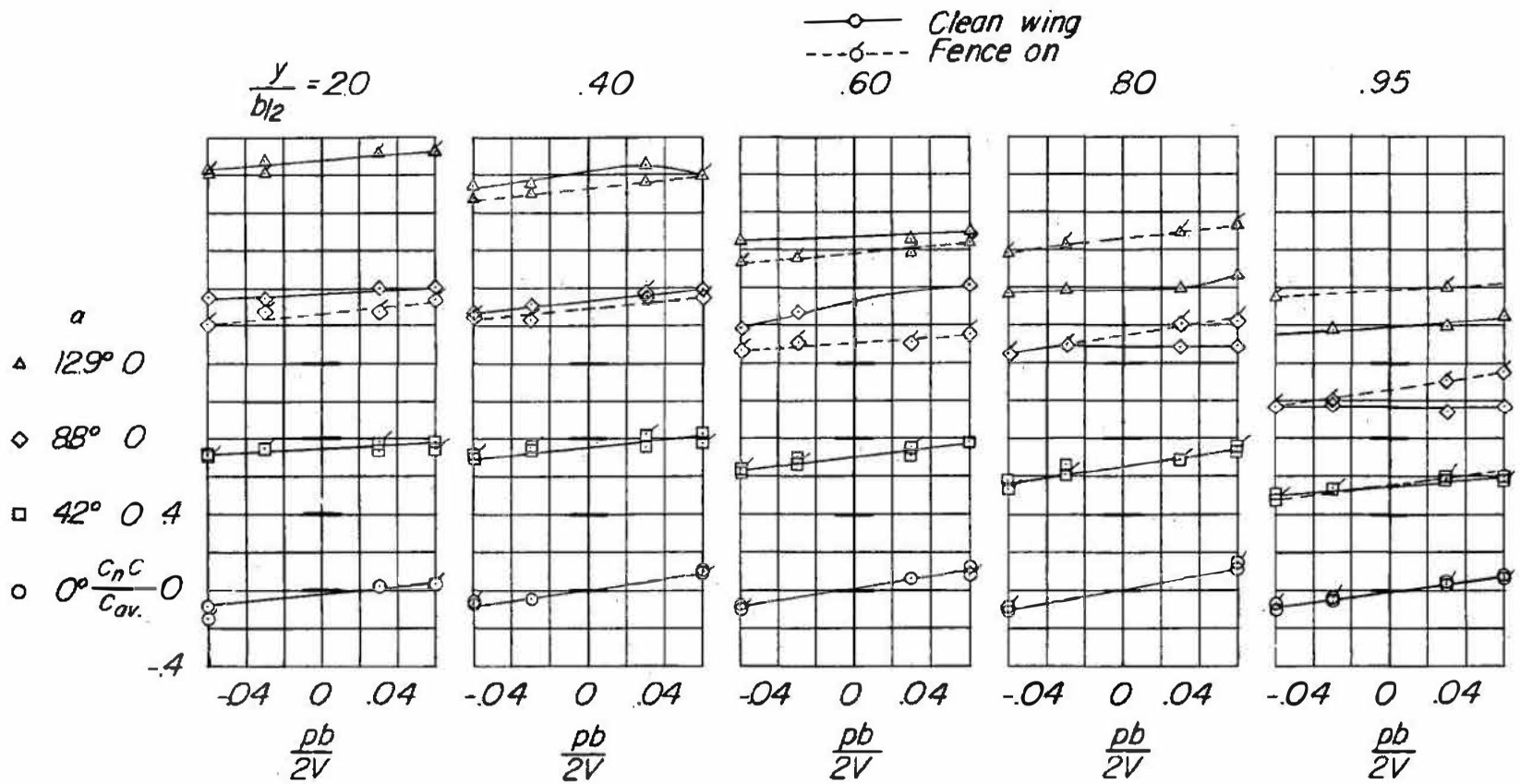

(b) M = 0.85; clean wing and wing with fence.

Figure 5.- Continued.

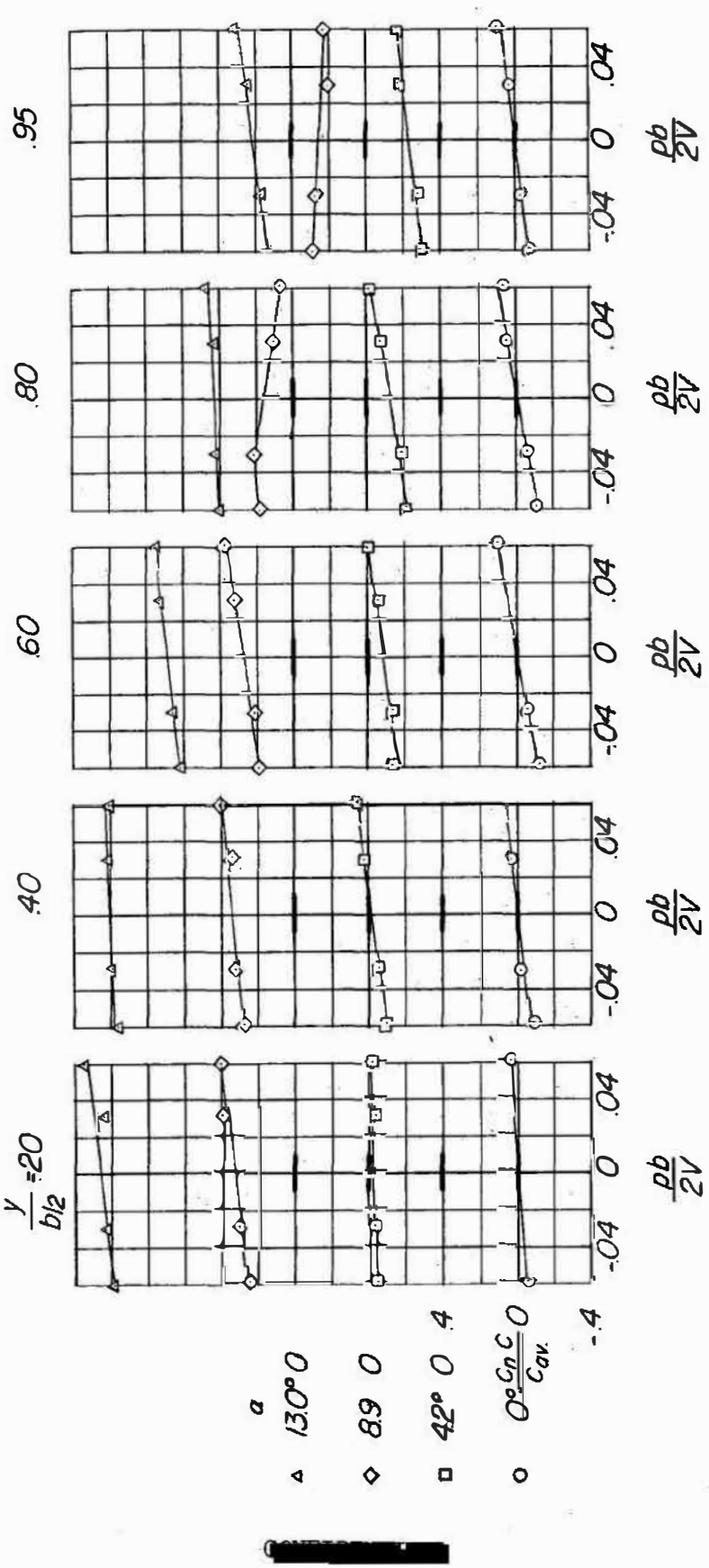

(c) M = 0.91; clean wing.

Figure 5.- Concluded.

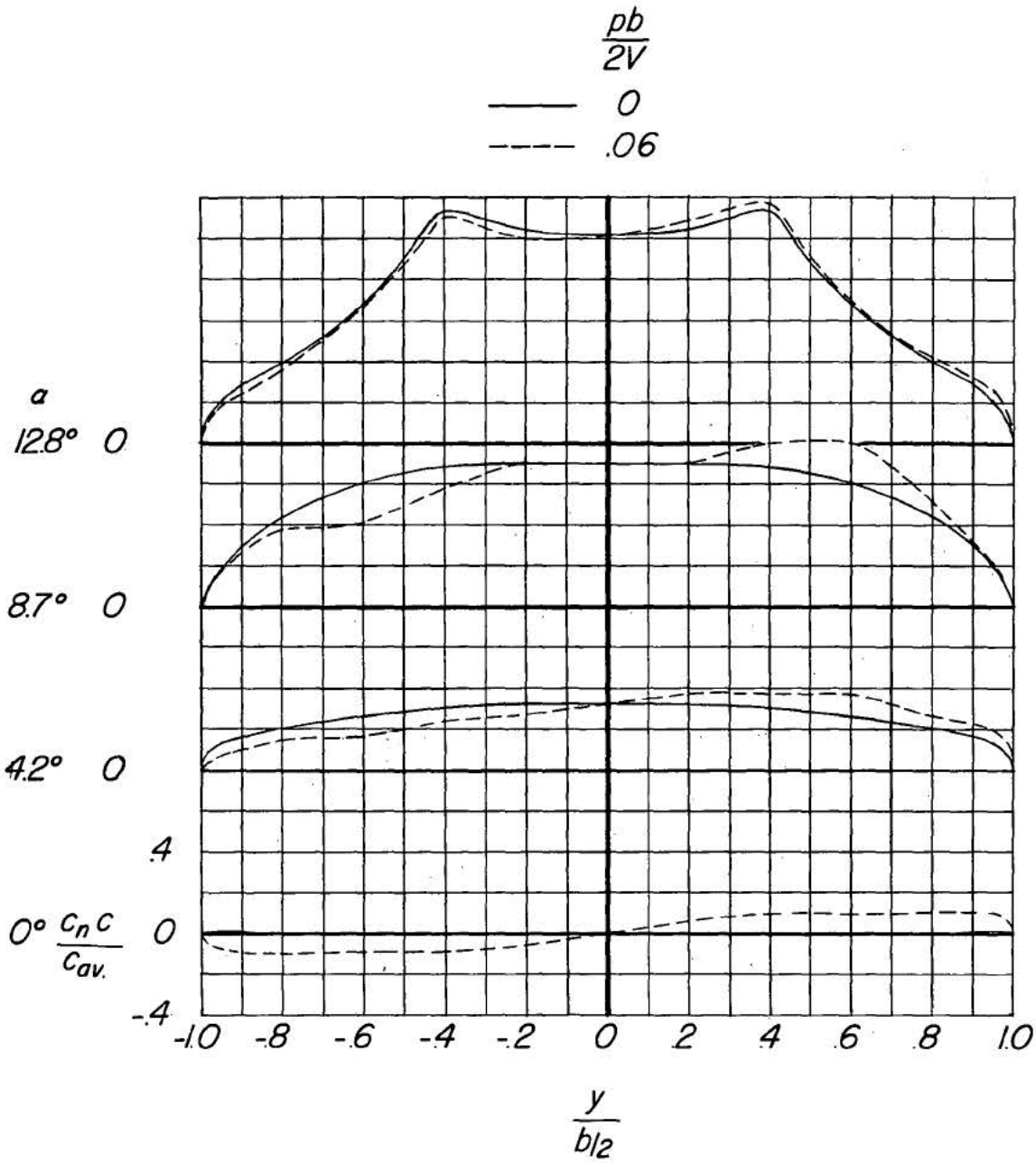

(a) M = 0.70; clean wing.

Figure 6.- Effect of rolling velocity on the span load distribution.

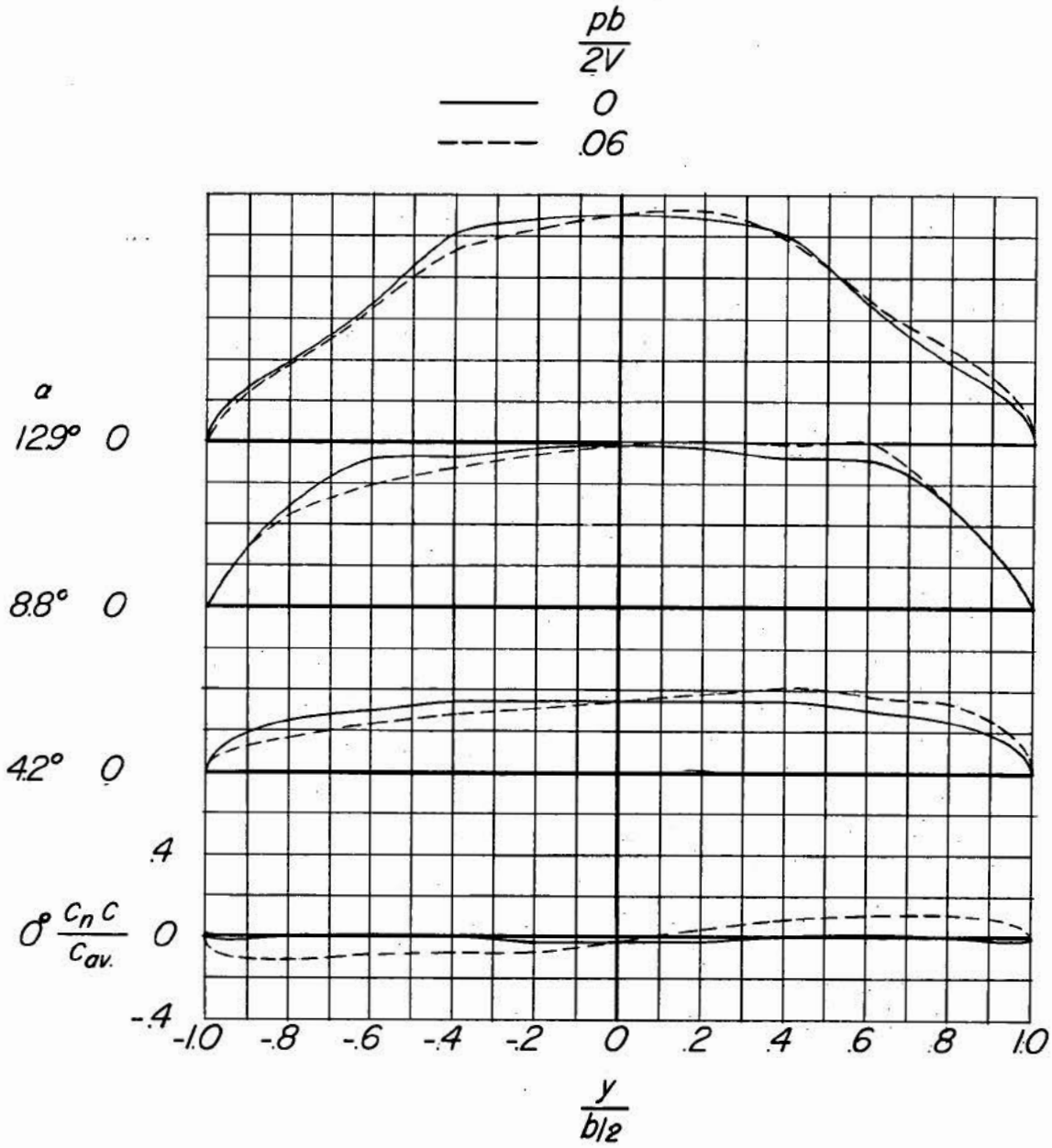

(b) M = 0.85; clean wing.

Figure 6.- Continued.

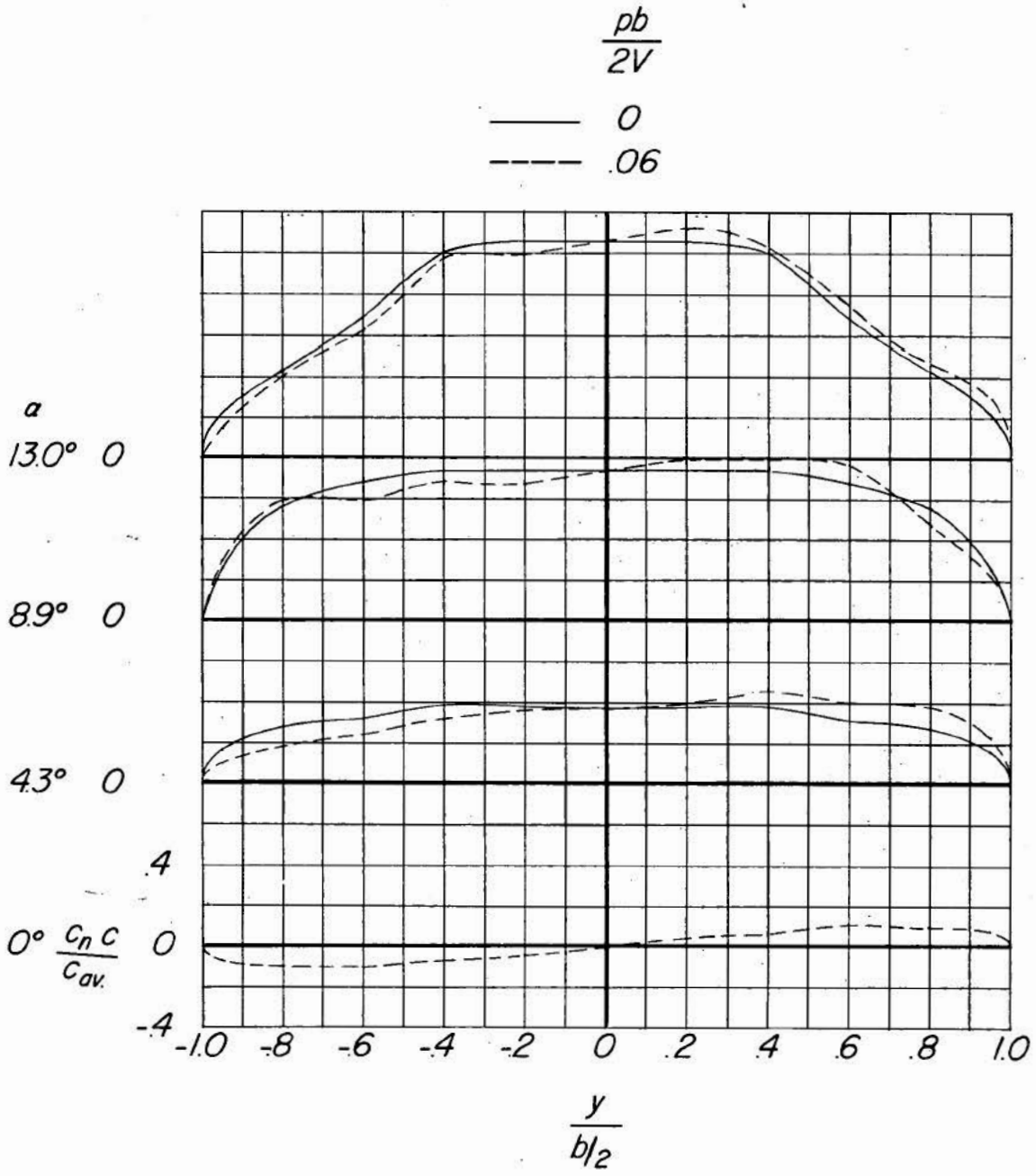

(c) M = 0.91; clean wing.

Figure 6.- Continued.

[redacted]

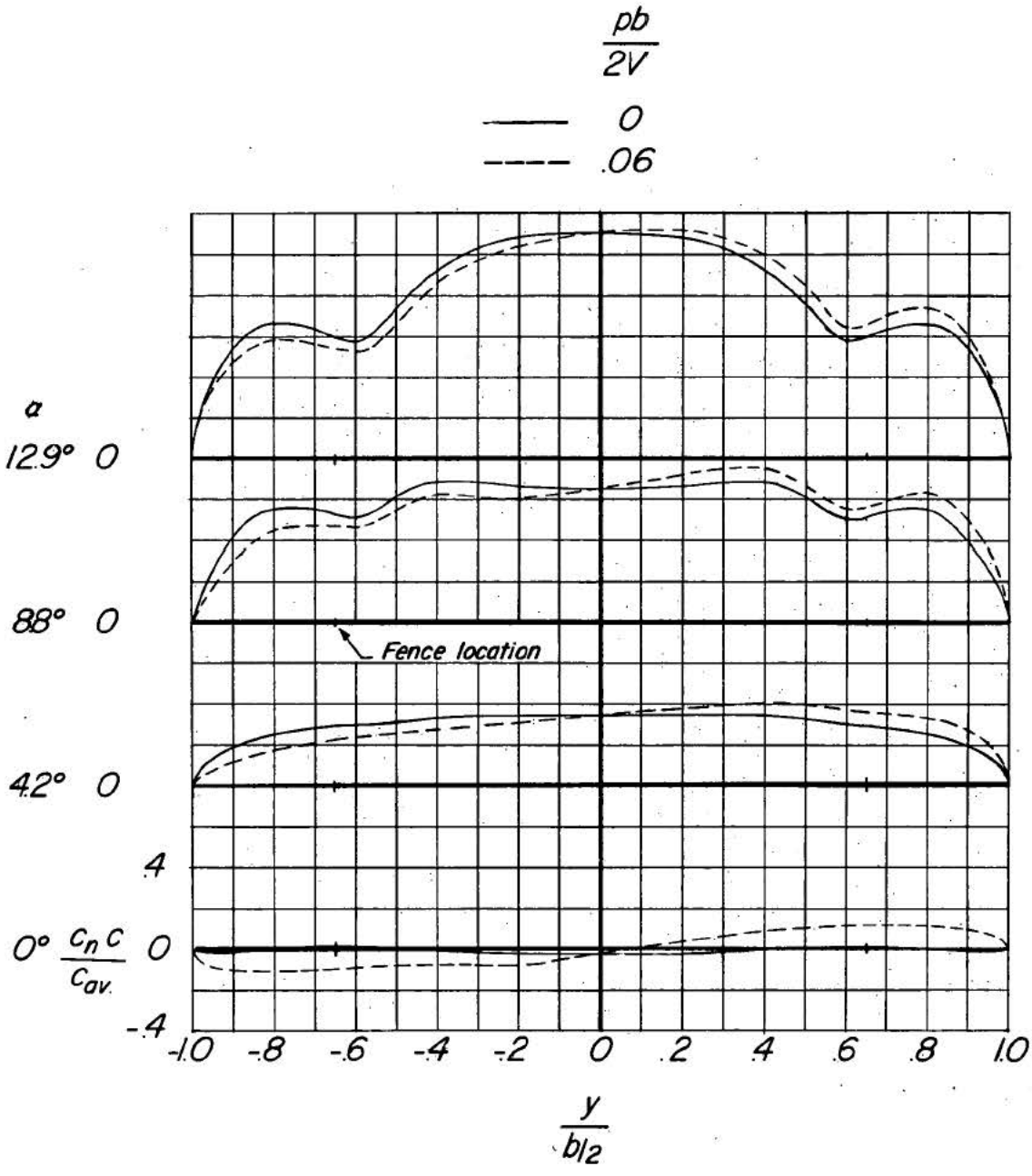

(d) M = 0.85; fence on.

Figure 6.- Concluded.

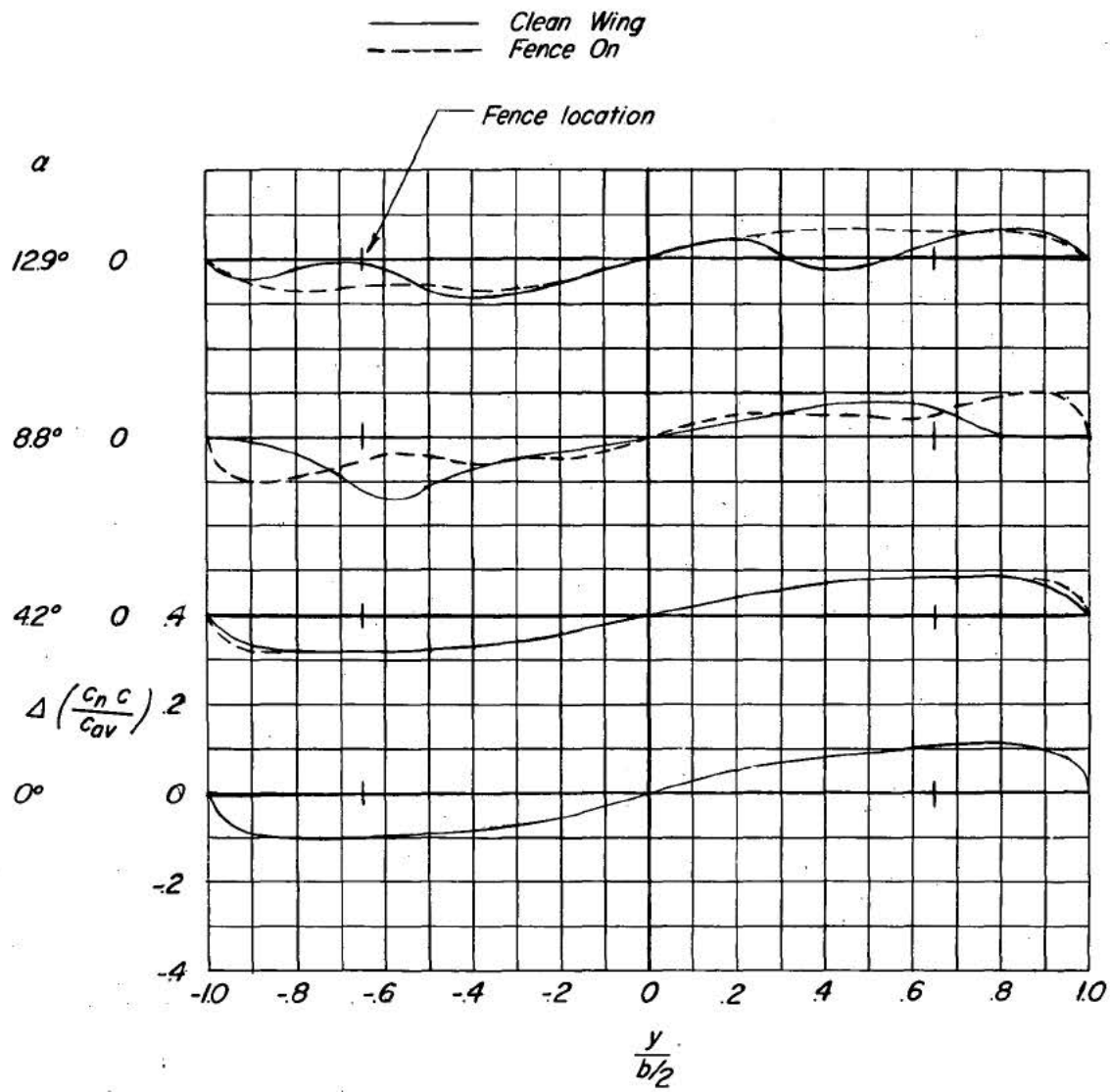

Figure 7.- Effect of the fence on the increment of load distribution due to roll. $\frac{pb}{2V} = 0.06$; M = 0.85.

[redacted]

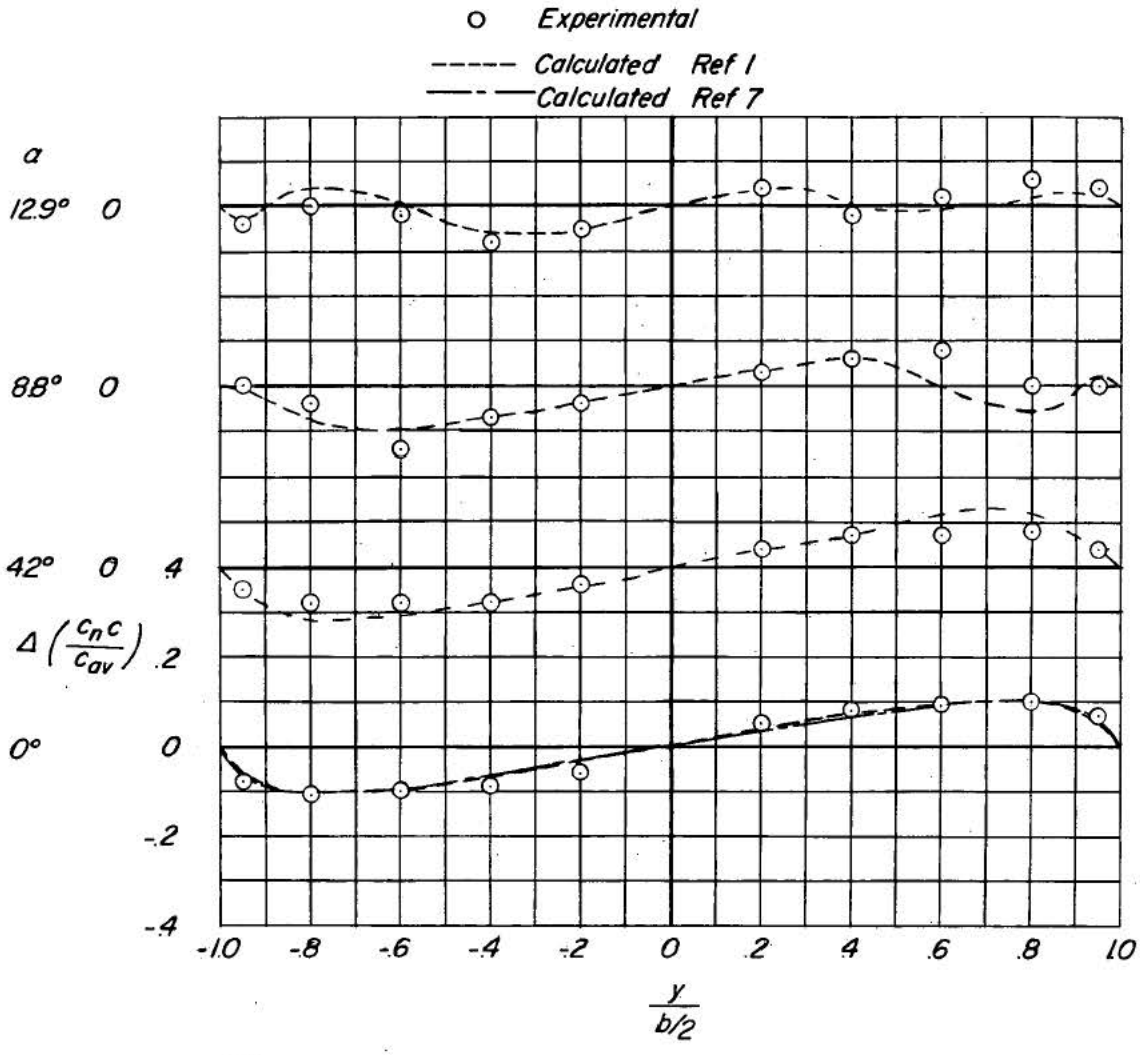

Figure 8.- Comparison of the measured and estimated increment of load distribution due to roll. $\frac{pb}{2V} = 0.06$; M = 0.85.

[redacted]

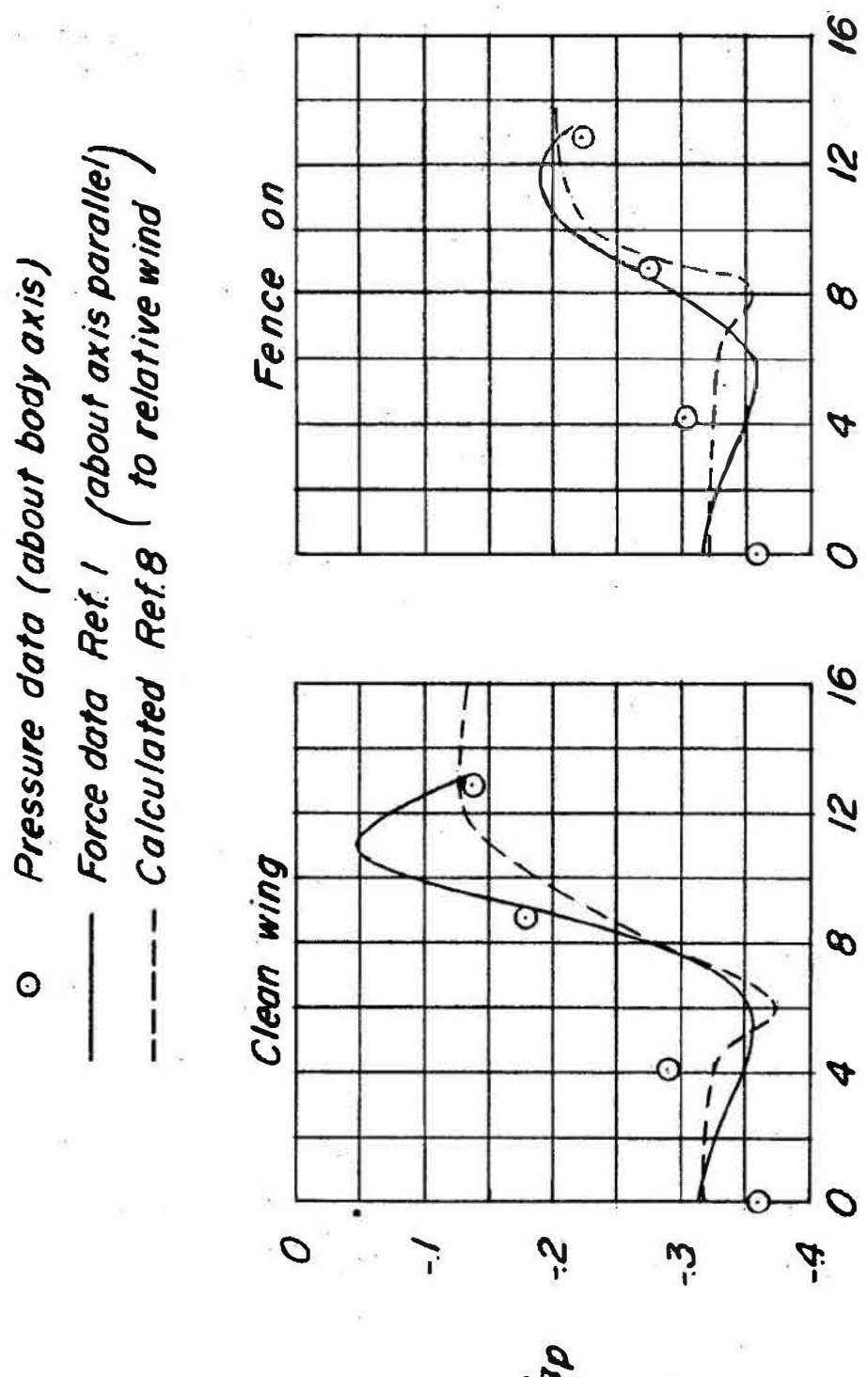

Figure 9.- Comparison of measured and calculated variation of C_{l_p} with angle of attack. M = 0.85.